CRYSTAL GROWTH & DESIGN
2006
VOL. 6, NO. 9
2149−2154

Impact of Evaporation Rates of Cd and Te on Structural, Morphological, Optical, and Electrical Properties of CdTe Thin Films Deposited by a Two-Sourced Evaporation Technique

A. Ali,[†] N. A. Shah,[†] A. K. S. Aqili,[‡] and A. Maqsood*,[†]

Thermal Physics Laboratory, Department of Physics, Quaid-i-Azam University, Islamabad 45320, Pakistan, and Physics Department, The Hashemite University, Zarqa, Jordan

Received April 13, 2006; Revised Manuscript Received June 30, 2006

ABSTRACT: A two-sourced evaporation technique was used for deposition of cadmium telluride thin films onto scratch-free transparent glass substrates, using Cd and Te as two different evaporants. Nine samples were deposited at three Te evaporation rates, that is, 6.5, 4.5, and 2.5 nm/s as a function of three substrate temperatures at 400, 300, and 200 °C respectively, keeping the Cd evaporation rate fixed at 2.7 nm/s. All the samples were characterized by X-ray diffraction (XRD) and scanning electron microscope (SEM), optically by Lambda 900 UV/vis/NIR spectrophotometer and electrically, that is, DC electrical resistivity, by the van der Pauw method at room temperature. Content composition was investigated by energy-dispersive X-ray analysis. Strong mutually supporting effects on structure, morphology, optical transmission, reflection, and electrical resistivity were observed.

1. Introduction

CdTe has emerged as a promising thin film material for a number of reasons. Thin films of CdTe are usually p-type semiconductors. Its 1.5 eV direct band gap is nearly ideal for terrestrial energy conversion.[1−6] It has a very high absorption coefficient, meaning that relatively thin layers can be used to make functional devices. Cadmium telluride has been used to make photovoltaic devices for quite some time. Many different CdTe devices have been fabricated in a number of different configurations. CdTe is a semiconductor that can be made both p-type and n-type.[7−9] By 1982, Kodak researchers Tyan and Perez-Albuerne had produced the first cell with 10% efficiency.[10] Subsequent refinement of the structure succeeded in device efficiencies of over 16.5%.[11−13] CdTe polycrystalline absorber layers have been deposited by a number of techniques. Specifically, device-quality films have been grown by sintering,[14] metal−organic chemical vapor deposition (MOCVD),[15−17] vapor-phase epitaxy,[18] screen printing,[19,20] electrodeposition,[21,22] spray pyrolysis,[23] elemental[24] and compound[25] vacuum evaporation, vapor transport deposition (VTD),[26,27] closed-space sublimation (CSS),[28] and two-sourced evaporation technique.[29]

In this paper, we investigate the deposition of CdTe films at three different Te evaporation rates as a function of three different substrate temperatures, keeping the Cd evaporation rate constant. We put in an effort to correlate their mutually interdependent structural, morphological, optical, and electrical properties.

2. Experimental Section

Cadmium, granulated about 3−6 mm, from BDH chemicals of Poole, England, and tellurium powder, −325 mesh, 99.998% (metals basis), from Alfa Aesar company were used as two-sourced materials inside an Edwards E306A vacuum system. The materials were loaded into two cylindrical graphite boats, with a hole of ∼2 mm diameter on the top to act as point sources and tightly wrapped around by 100 A tungsten wire. The boats were heated indirectly by passing current through the Cd and Te heaters. The temperature controllers with K-type thermocouples (Chromel & Alumel, −270 to 1350 °C, sensitivity ∼41 μV/°C) inserted into the rear of the graphite boats were used to maintain the evaporation temperatures of Cd and Te within ±1 °C of the required temperature range. Scratch-free transparent glass substrates of visibly good surface finish of area 5 cm × 5 cm were cleaned for 3 h in a pure IPA bath (isopropyl alcohol from MERCK company), in an ultrasonic cleaner from Cole Parmer company, model 8890E-DTH. The substrate was placed over the stainless steel substrate holder; while the infrared heater was used to heat the substrate fixed at a distance of about 15 cm from the source materials, a third K-type thermocouple was placed over the substrate for temperature control during the evaporation as shown in Figure 1. The chamber was then closed and allowed to evacuate with the help of rotary and diffusion pumps attached to a liquid nitrogen trap. The chamber was evacuated to around 10^{-6} mbar. The vacuum during the evaporation was ∼1.5×10^{-5} mbar. The thickness of the film and the deposition rate were measured with the help of a quartz crystal film thickness monitor, model FTM7 from Edwards BOC, England, fixed near the film. For the deposition of film I, substrate temperature was kept at 400 °C for 1 h before deposition of film. The source materials were sintered for 5 min before opening the shutter to have a stable and constant evaporation rate. In the first step, the Cd and Te source temperatures were 400 and 510 °C respectively, which were precalibrated. Deposition time was around

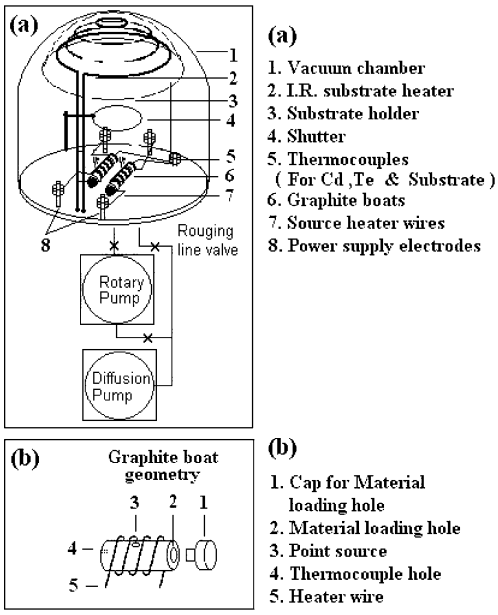

Figure 1. Two-source evaporation unit fabricated at Thermal Physics Laboratory.

* E-mail: tpl.qau@usa.net. Tel: +92512828187. Fax: +92519210256.
[†] Quaid-i-Azam University.
[‡] The Hashemite University.

10.1021/cg060217q CCC: $33.50
Published on Web 07/29/2006

Table 1. The Deposition Parameters and Optical and Electrical Characteristics for the Studied Samples[a]

		Cd			Te						
Sl no.	T_{sub} (°C)	T_{ev} (°C)	rate (nm/s)	wt %	T_{ev} (°C)	rate (nm/s)	wt %	d (nm)	σ (nm)	E_g (eV)	R_s (Ω/sq)
I	400	400	2.7	47.21	510	6.5	52.79	600	13	1.486	4.29×10^9
II	400	400	2.7	45.44	490	4.5	54.16	590	11	1.483	3.33×10^9
III	400	400	2.7	45.49	475	2.5	54.50	510	12	1.490	3.33×10^9
IV	300	400	2.7	45.49	510	6.5	54.51	510	24	1.493	5.03×10^9
V	300	400	2.7	44.48	490	4.5	55.52	660	17	1.502	3.33×10^9
VI	300	400	2.7	45.85	475	2.5	54.14	570	19	1.492	1.89×10^9
VII	200	400	2.7	49.55	510	6.5	50.45	~600			4.57×10^6
VIII	200	400	2.7	47.84	490	4.5	52.01	~650			4.72×10^6
IX	200	400	2.7	61.14	475	2.5	38.85	~700			3.03×10^3

[a] T_{sub} = substrate temperature; T_{ev} = source temperature; wt % = weight percent of component; d = film thickness; σ = film roughness; E_g = energy gap; R_s = sheet resistance at room temperature.

90 s, after which the shutter was closed and the films were left at the same substrate temperature for 20 min more; after that the substrate heater was switched off to allow cooling to 100 °C before opening the vacuum chamber. Similarly we repeated our experiment by changing only the Te evaporation temperature to 490 and 475 °C in two steps to get films II and III, respectively. This completes our first set of samples (I, II, and III) at 400 °C substrate temperature. By exactly repeating these effects for 300 and 200 °C substrate temperatures, we got a second set of samples (IV, V, and VI) and third set of samples (VII, VIII, and IX), respectively.

The deposition of CdTe films by direct combination of cadmium and tellurium vapors on the substrate surface is based on the following reversible reaction:

$$2Cd(g) + Te_2(g) \leftrightarrow 2CdTe(s)$$

The direct combination of elemental cadmium and tellurium vapors at the substrate surface has been used for the deposition.

Since the source boats of both the materials are similar, the most important parameter, which controls the evaporation rate and the re-evaporation from the substrate, is the vapor pressure of Cd and Te. The flux F_i of species i per unit area at the substrate surface is given by[30]

$$F_i = \frac{A_c P_i}{\pi d_s^2 \sqrt{2\pi m_i k_B T}}$$

where A_c is the area of the cell aperture, P_i is the equilibrium vapor pressure of species i in the cell at absolute temperature T, d_s is the distance of the boat from the substrate, m_i is the mass of effusion species i, and k_B is the Boltzmann constant. The vapor pressures of Cd and Te at various temperatures are given in refs 31 and 32. The structure of the films was studied by X-ray diffraction (XRD) using Cu Kα (1.5418 Å) radiation with operating conditions voltage/current 40 kV/30 mA. The microstructure and composition analyses of the samples were performed using a scanning electron microscope (SEM) with EDX, model JEOL 5910. The optical transmission between 300 and 2600 nm was recorded by Perkin-Elmer Lambda 900 UV/vis/NIR spectrophotometer with UV-Win Lab software. The electrical resistivity of cut samples with gold-coated contacts was determined according to van der Pauw geometry using Keithley 2410-C 1100 V source meter. Silver paste was used above the gold coating for ohmic contacts.

3. Results and Discussion

The deposition parameters and electrical characteristics for the studied samples are listed in Table 1. It is evident from the table that Te evaporates more slowly than Cd. A detailed discussion follows.

3.1. Structural Properties. The crystallinity of the samples deposited at three different Te rates as a function of substrate temperature were examined by X-ray diffraction as shown in Figure 2. All the samples were polycrystalline. The sharp diffraction peaks at $2\theta \cong 23.750°$, 39.286°, 46.433°, and 76.56° correspond to (111), (220), (311), and (511) planes of the cubic

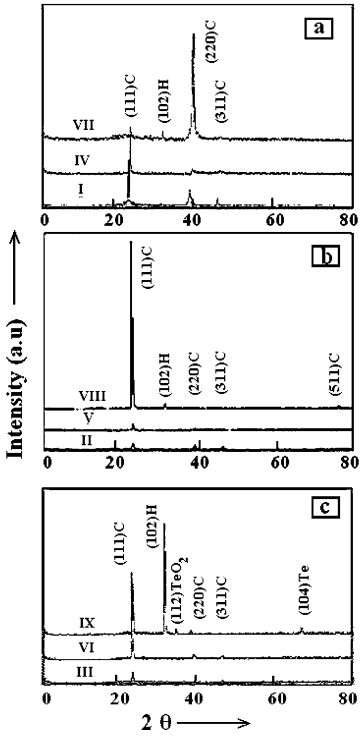

Figure 2. XRD patterns for CdTe films grown at different Te rates as a function of substrate temperatures: (a) 6.5; (b) 4.5; (c) 2.5 nm/s.

CdTe structure, which has the space group $F\bar{4}3m$ and lattice constant 6.481 Å (ICDD 15-0770). For 200 °C substrate temperature, a peak at $2\theta \cong 32.5°$ in samples VII, VIII, and IX corresponding to (102) plane of hexagonal CdTe structure (ICDD 19-0193) appeared. Two additional peaks at $2\theta \cong 35.52°$ and 67.34° in Figure 2c for sample IX corresponding to (112) and (104) planes of tetragonal TeO_2 (ICDD 11-6 93) and hexagonal Te (ICDD 4-554) structures appeared, respectively.

It is clear from XRD intensity variation in Figure 2 that for samples I, II, and III at 400 °C and IV, V, and VI at 300 °C substrate temperatures that any change in Te evaporation rate results in a minor reorientation of planes where as for samples VII, VIII, and IX at lower substrate temperature of 200 °C, Te evaporation rate changes the dominant plane as is evident from the different dominant planes, and also new phases of Te and TeO_2 appeared.

The presence of hexagonal tellurium phase in sample IX may be due to low the evaporation rate as well lower substrate temperature of 200 °C. The formation of TeO_2 may be due to the reaction of Te with the oxygen present in the glass substrate, which already contains so many oxides and phases; besides it

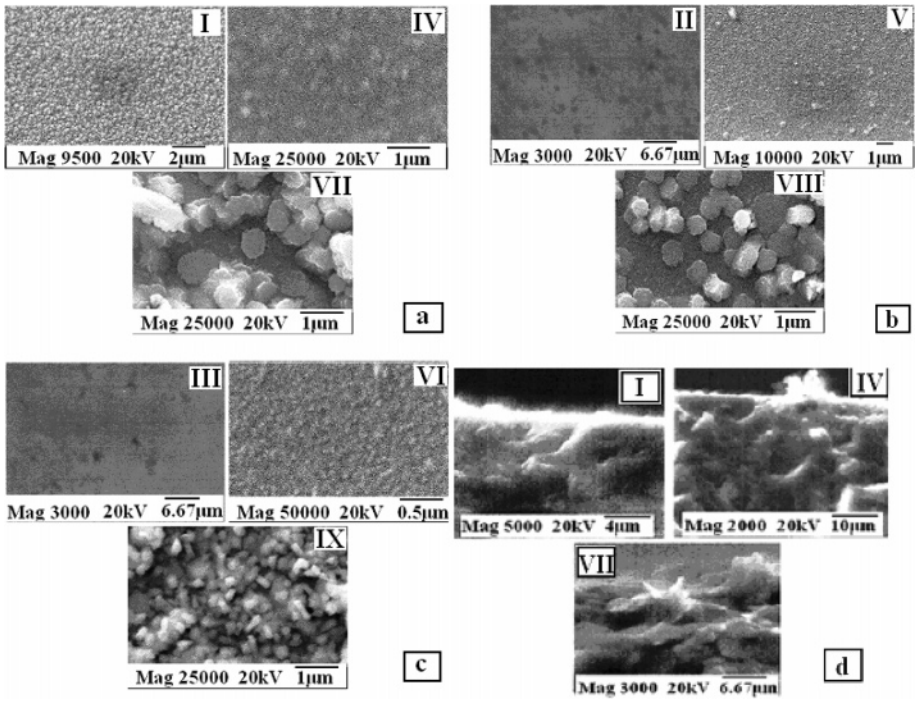

Figure 3. Plan-view SEM images of CdTe showing film morphology at different Te evaporation rates, (a) 6.5, (b) 4.5, and (c) 2.5 nm/s, and cross-sectional SEM image showing film morphology (d) at Te evaporation rate of 6.5 nm/s.

is also possible that TeO_2 may have resulted after the deposited samples were taken out of vacuum chamber in open room environment for conducting different analyses where loosely placed Te has a fair chance of oxidation in open atmosphere. This made the formation of a single-phase CdTe compound more difficult. Similar observations were also reported earlier.[33] The absence of tellurium phase for samples I−VI is due to the higher substrate temperatures of 400 and 300 °C. It can be observed that by coevaporating Cd and Te at higher substrate temperatures single-phase CdTe films can be achieved.

Scanning electron microscope (SEM) images for three different Te evaporation rates, as a function of substrate temperature, are shown in a series of photographs displayed in Figure 3. Although the deposited films were uniform macroscopically, we can see relatively dark and light gray regions in the SEM images for all the films. These are diffraction effects due to a small thickness gradient in thin films caused by radial temperature gradients in the substrate surface during the deposition. The dark areas in the images correspond to the rough surface. In contrast, the light gray regions were relatively smooth and correspond to the coalesced film structure. As the substrate temperature increased, a dense coalesced film structure resulted.[34] There was significant variation in morphology, which was mainly attributed to substrate temperature as shown in plan-view images of Figure 3 with completely different features, more clear in the magnification range mentioned in scale on images. The evolution of these features is displayed in side view images of films in Figure 3d, which clearly indicates that despite nearly same weight percent of Cd and Te in films I, IV, and VII listed in Table 1, a more solid coalesced uniform structure is formed in film I, which has shifted toward less coalescesed structure in film IV because one can see some loosely placed particles besides a solid region, and in film VII, this has transformed into simply piled up particles stacked on one another resulting in a rough surface. This gives a good feeling about the deposition of Cd and Te on the film surface at the same Te evaporation rate and different substrate temperatures.

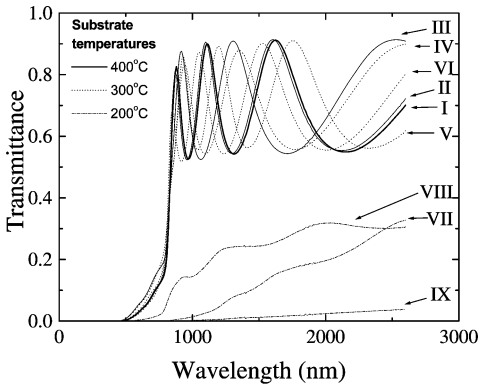

Figure 4. Normal incidence transmittance spectra for CdTe thin layers grown on glass substrate.

3.2. Optical Properties. Optical transmittance and reflectance spectra for CdTe samples between 300 and 2500 nm were recorded by spectrophotometer as shown in Figures 4 and 5, respectively. It is clear from transmittance for different Te rates that samples I, II, and III deposited at 400 °C and samples IV, V, and VI at 300 °C substrate temperatures are more transparent, and their interference pattern shows that they are more uniform. The spectral behavior of these films shows that above $\lambda = 800$ nm, that is, at longer wavelengths, $T + R = 1$. This indicates that for such films neither absorption nor scattering of light occurs beyond the absorption edge as shown for one of the samples in Figure 6. The appearance of maxima and minima occurs from the interference effect, and their number increases with increasing film thickness.[35,36] The transmittance and reflectance of films VII, VIII, and IX at 200 °C substrate temperature show nonuniform rough surfaces for which $T + R \neq 1$. This indicates that scattering losses are present. There is also no sharp band edge.

The optical properties such as film thickness, refractive index, absorption coefficient, and optical band gap were calculated from the transmission spectra. Due to the effect of surface

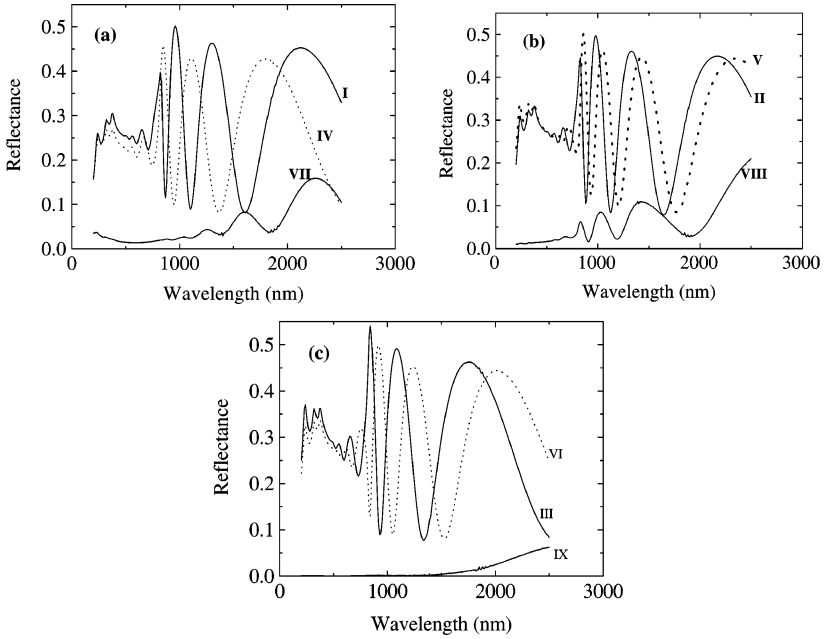

Figure 5. Normal incidence reflectance spectra for CdTe thin layers grown on glass substrate.

roughness on the transmission of the films, transmission formula,[37] which includes the roughness, was used as

$$T = \frac{A_1 \exp(\alpha d)}{B_1 \exp(2\alpha d) + C_1 \exp(\alpha d) + D_1} \frac{B_2 \exp(2\alpha d) + C_2 \exp(\alpha d) + D_2}{B_2 \exp(2\alpha d) + C_3 \exp(\alpha d) + D_3} \quad (1)$$

where

$$A_1 = \gamma^2[16 n_1 n_3 (1-\rho)(n_2^2 + k_2^2)U], \qquad B_1 = st - \rho s v U^2, \quad B_2 = st$$

$$C_1 = \beta\{[2(4n_3k_2^2 - ZY)\cos\phi + 4k_2(n_3Y + Z)\sin\phi] - \rho U^2[4k_2(Z - n_3Y)\sin\phi - 2(ZY + 4n_3k_2^2)\cos\phi]\}$$

$$C_2 = \beta\{2(4n_3k_2^2 - ZY)\cos\phi + 4k_2(n_3Y + Z)\sin\phi\}, \qquad C_3 = \eta\{2(4n_3k_2^2 - ZY)\cos\phi + 4k_2(n_3Y + Z)\sin\phi\}$$

$$D_1 = \beta^2[uv - \rho t u U^2], \quad D_2 = \beta^2[uv], \quad D_3 = \eta^2[uv], \qquad u = (n_1 - n_2)^2 + k_2^2, \quad v = (n_2 - n_3)^2 + k_2^2$$

$$s = (n_1 + n_2)^2 + k_2^2, \quad t = (n_2 + n_3)^2 + k_2^2, \qquad Y = n_2^2 - n_1^2 + k_2^2, \quad Z = n_2^2 - n_3^2 + k_2^2$$

$$\rho = [(n_1 - n_3)^2 + k_3^2]/[(n_1 + n_3)^2 + k_3^2], \qquad n_3 = n_1[1/T_s + (1/T_s^2 - 1)^{1/2}]$$

$$\eta = \exp[-2(2\pi\sigma/\lambda)^2 n_1^2], \quad \beta = \exp[-2(2\pi\sigma/\lambda)^2 n_2^2], \qquad \gamma = \exp\left[-\frac{1}{2}(2\pi\sigma/\lambda)^2(n_1 - n_2)^2\right]$$

$$U^{-1} = \frac{(1-\rho)^2}{2T_s} + \left[\frac{(1-\rho)^4}{4T_s^2} + \rho^2\right]^{1/2}, \quad U = \exp(-\alpha_s d_s)$$

T_s is the transmittance of the substrate, and for transparent substrate, $U = 1$ and $k_3 = 0$, n_i is the real part and k_i is the imaginary part (extinction coefficient) of the complex refractive index of air (n_1, k_1), film (n_2, k_2), and substrate (n_3, k_3), and σ is the rms height of surface irregularity (roughness).

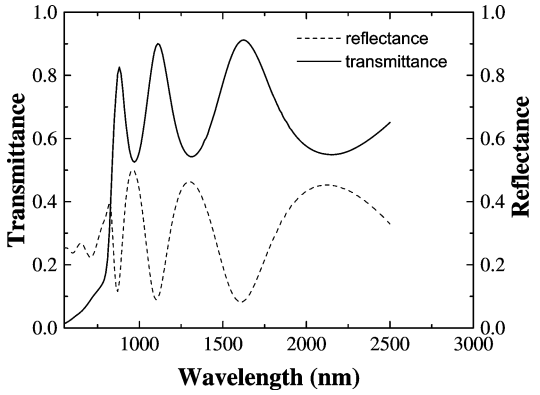

Figure 6. Comparison of normal incidence transmittance and reflectance spectrum for a typical CdTe thin film sample I grown on glass substrate.

Equation 1 can be solved numerically for d and σ using consecutive maximum and minimum and numbering the interference order to find the value of n all over the spectra; more details on the method of calculation are given elsewhere.[37]

However the above formula cannot be used for doped films where the reduction in transmission is due to both the roughness and the internal absorption. For that reason, fitting of an approximate formula[35,37] was used.

$$T = \frac{Ax}{B - Cx\cos(\phi) + Dx^2} \quad (2)$$

Here T is the normal transmittance for the system consisting of a thin film on a transparent substrate surrounded by air (refractive index = 1) and taking into account all multiple reflections at the interface for the case of $k^2 \ll n^2$, which is true for this kind of semiconductor thin films. The other variables are defined as: $A = 16\,n^2 s$, $B = (n+1)^3(n+s^2)$, $C = 2(n^2-1)(n^2-s^2)$, $D = (n-1)^3(n-s^2)$, $\phi = 4\pi nd/\lambda$, $x = \exp(-\alpha d)$, and $k = \alpha\lambda/(4\pi)$. Here n and s are the refractive

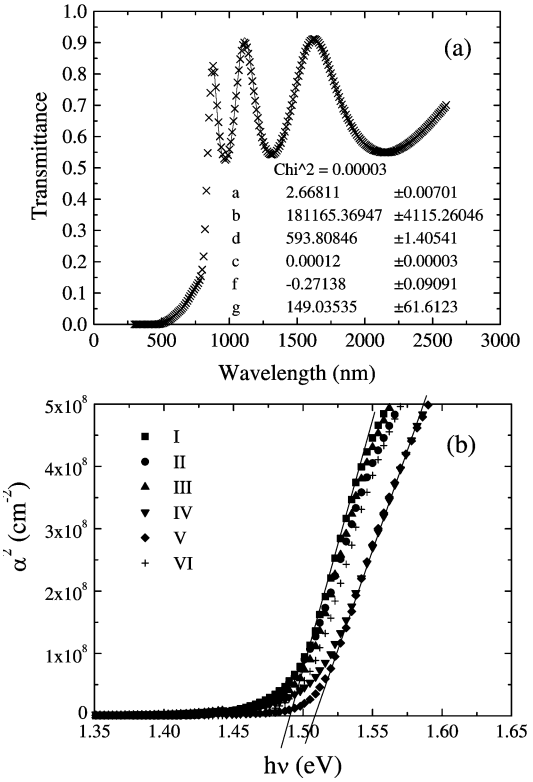

Figure 7. Transmittance of sample I as a function of wavelength with fitting (a) and plot of α^2 versus photon energy ($h\nu$) for samples I−VI prepared at 400 and 300 °C substrate temperatures (b).

indices of the film and the substrate, respectively, d is the thickness of the film, α is the absorption coefficient of the film, and λ is the wavelength.

Here n varies as

$$n = a + \frac{b}{\lambda^2} \tag{3}$$

and polynomial approximation for α is

$$\alpha = c + \frac{f}{\lambda} + \frac{g}{\lambda^2} \tag{4}$$

where a, b, c, g, and f are constants obtained from the fitting of the transmission spectra. The fitting parameters c, f, and g are good for the transparent region only where the values of α are very small and varying slowly with λ. In the medium and high absorption regions, we can calculate α by using the values of n and d from the fitted curve and the exact value of x. The exact solution of eq 2 for x is

$$x = \frac{(C' + A/T) - [(C' + A/T)^2 - 4BD]^{1/2}}{2D} \tag{5}$$

where $C' = C \cos \varphi$. Then $\alpha = -ln(x)/d$. The values of n and d were taken from the transmittance as stated above. If photon energy is above the optical band-gap energy, the loss of transmittance due to the absorption is much more than that of light scattering due to film roughness, so eq 5 can be used with a good precision.

One such fitted transmission spectra, using eq 2, is shown in Figure 7a. The difference of the thickness calculated by solving eq 1 and that by fitting eq 2 is ∼1−2%, which is due to ignoring roughness in eq 2. The direct band gap of the films was determined using the well-known relation for the direct band gap, $\alpha h\nu = A'(h\nu - E_g)^{1/2}$, where A' is a constant, $h\nu$ is the photon energy, and E_g is the optical band energy gap.[28] Energy gap E_g was obtained by extrapolating the $(\alpha h\nu)^2$ vs the incident photon energy ($h\nu$) plot, a slight shift of energy gaps was noticed as mentioned in Table 1. Figure 7b shows the plot of α^2 versus photon energy ($h\nu$) for samples I−VI. The optical energy gaps, along with other optical parameters, are tabulated in Table 1. The optical energy gaps are close to that reported for crystalline CdTe material, which ensured the good quality of the prepared films.

The results in Table 1 and Figures 4−7 indicate that the films prepared at substrate temperature of 400 °C were uniform and in most of the cases did not depend on the evaporation rate, but the effect of the substrate temperatures was dominant. However films prepared at substrate temperature of 300 °C were more sensitive to the change of evaporation rate of Te. The high absorption of the films prepared at substrate temperature of 200 °C indicated that CdTe compound was not fully formed, and the films contained a mixture of Cd and Te elements. This matches the XRD results.

3.3. Electrical Properties. The direct method of measuring DC electrical resistivity, ρ_{dc}, or sheet resistance, R_s, is to prepare a rectangular sample of film and measure its resistance.[38] It is necessary to ensure that the two gold-coated contacts at the two ends of the rectangle are ohmic or as close to ohmic as possible so that the bulk resistivity, not the contact resistance, is measured. R_s of squarely cut samples is independent of the size of the square and depends only on resistivity and thickness, d, of films, that is, $R_s = \rho_{dc}/d$. Van der Pauw resistivity measurements were performed on squarely cut samples of 10 mm length per side provided with four symmetrically spaced gold-coated contacts. For the electrical measurements, very low resistance silver wires and contacts were used. These were performed at room temperature. Van der Pauw correction factors were chosen from a graph.[38] Film thicknesses were determined by curve fitting of optical transmission data. It can be seen in Table 1 that R_s of the samples I−VI deposited at ≥300 °C substrate temperature is very high, $\sim 10^9$ Ω/sq. When the tellurium to cadmium molar ratio in the reaction mixture is increased slightly, the film becomes p-type, and when the tellurium-to-cadmium ratio is reduced slightly, n-type CdTe results (cadmium vacancies and tellurium vacancies are acceptors and donors, respectively). This transition from p-type to n-type CdTe occurs over a very narrow range of the tellurium-to-cadmium molar ratio in the reaction mixture. In case of samples VII and VIII at 200 °C substrate temperature, though the Cd and Te ratios are not much different, the R_s is much less, in the range of $\sim 10^6$ Ω/sq, which could be due to the low growth of CdTe compound between Cd and Te atoms at low substrate temperature. In case of sample IX, the R_s value falls to 10^3 Ω/sq, which is due to the presence of excessive Cd (∼61 wt %) at low substrate temperature as is evident from Table 1. Similar observations about resistivity of polycrystalline CdTe films were reported earlier according to which the lowest resistivity obtainable was about 200 Ω cm.[39]

4. Conclusion

A two-sourced evaporation technique was found useful for controlled deposition of CdTe thin films. At high substrate temperatures of 400 and 300 °C, coevaporated Cd and Te resulted in polycrystalline single-phase CdTe thin films. These films were hard and transparent (above 800 nm band edge) and had high resistivity. Different evaporation rates of Te showed

no significant change. At low substrate temperature of 200 °C new phases of Te and TeO_2 appeared along with CdTe, and the films deposited had rough surfaces, were less transmissive, and also had low resistivity. The Te evaporation rates showed significant change of dominating planes in the XRD structure and also affected the transmittance, reflectance, and resistivity of the deposited films. These CdTe films can be used in the field of compound semiconductor imaging detectors specially for nuclear medicine and X-ray astronomy applications.

Acknowledgment. The author Abid Ali acknowledges the able role of Higher Education Commission (HEC), Islamabad, Pakistan, for financial support for Ph.D studies through Merit Scholarship. This research was also partly supported through the funds provided by Pakistan Science Foundation Project No. PSF/RES/C-Qu/Phys 121. The authors also appreciate the valuable discussion with Dr. M. Anis-ur-Rehman, Mr. Saifullah Awan, and Mrs. Naghma Haider.

References

(1) Loferski, J. J. *J. Appl. Phys*. **1956**, *27*, 777.
(2) Chu, T. L.; Chu, S. S.; Firszt, F.; Naseem, H. A.; Stawski, R. *J. Appl. Phys*. **1985**, *58* (3), 1349.
(3) Britt, J.; Ferekides, C. *J. Appl. Phys.* **1993**, *62*, 285.
(4) Chu, T. L.; Chu, S. S.; Han, K. D.; Han, Y. X.; Liu Y. H.; Mantravadi, M. K. *Sol. Cells* **1988**, *24*, 27.
(5) Touskova, J.; Kindl, D.; Kovanda, J. *Thin Solid Films* **1992**, *214*, 92.
(6) Han, B. W.; Park, S. C.; Ahn, J. H.; Ahn, B. T. *Sol. Energy* **1998**, *64*, 49.
(7) Basol, B. M.; Ou, S. S.; Stafsudd, O. M. *J. Appl. Phys*. **1985**, *58* (10), 3809.
(8) Zweibel, K. P.; Moskowitz, P.; Fthenakis, V. Thin-Film Cadmium Telluride Photovoltaics: ES&H Issues, Solutions, and Perspectives. NREL/TP-520-24057, DE-AC36-99-G010337. National Renewable Energy Laboratory: Golden, Colorado, 1998.
(9) Kazmerski, L. L. *29th IEEE Photovoltaics Specialists' Conf*. **2002**, 21.
(10) Tyan, Y.S.; Perez-Albuerne, E. A. *16th IEEE Photovoltaic Specialists' Conf*. **1982**, 794.
(11) Wu, X.; Keane, J. C.; Dhere, R. G.; Dehart, C.; Albin, D. S.; Duda, A.; Gessert, T. A.; Asher, S.; Levi, D. H.; Sheldon, P. In *Seventeenth European Photovoltaic Solar Energy Conference, Proceedings of the International Conference*; WIP-Munich and ETA: Florence, Italy, 2001; Vol. 1, p 995.
(12) Britt, J.; Ferekides, C. *Appl. Phys. Lett*. **1993**, *62* (22), 2851.
(13) Ohyama, H.; Aramoto, T.; Kumanzawa, S.; Higuchi, H.; Arita, T.; Shibutani, S.; Nishio, T.; Nakajima, J.; Tsuji, M.; Hanafusa, A.; Hibino, T.; Omura, K.; Morozono, M. *26th IEEE Photovoltaic Specialists Conf*. **1997**, 343.
(14) Jun, Y.K.; Im, H. B. *J. Electrochem Soc*. **1988**, *27* (7), 1658.
(15) Chou, H.C.; Rohatgi, A.; Jokerst, N. M.; Kamra, S.; Stock, S. R.; Lowrie, S. L.; Ahrenkiel, R. K.; Levi, D. H. *Mater. Chem. Phys.* **1996**, *43*, 178.
(16) Chu, T.L.; Chu, S. S.; Ferekides, C.; Britt, J.; Wu, Q. *J. Appl. Phys*. **1991**, *69* (11), 7651.
(17) Rohatgi, A.; Summers, C.J.; Erbil, A. *Proc. Polycryst. Thin Film Program Rev. Meet*. **1989**, 45.
(18) Yamaguchi, K.; Nakayama, N.; Matsumoto, H.; Ikegami, S. J. *J. Appl. Phys.* **1977**, *16* (7), 1203.
(19) Uda, H.; Matsumoto, H.; Komatsu, Y. *16th IEEE Photovoltaics Specialists Conf*. **1982**, 801.
(20) Matsumoto, H.; Kuribayashi, K.; Uda, H.; Komatsu, Y.; Nakano, A.; Ikegami, S. *Sol. Cells* **1984**, *11*, 367.
(21) Basol, B. M.; Tseng, E. S.; Rod, R. L.; Ou, S. S.; Stafsudd, O. M. *16th IEEE Photovoltaic Specialists Conf*. **1982**, 804.
(22) Meyers, P. V. *Sol. Cells* **1988**, *24*, 35.
(23) Serreze, H. B.; Lis, S.; Squillante, M. R.; Turcotte, R.; Talbot, M.; Entine, G. *15th IEEE Photovoltaics Specialists Conf*. **1981**, 1068.
(24) Yi, X.; Wang, L.; Mochizuki, K.; Zhao, X. *J. Phys. D: Appl. Phys*. **1988**, *21*, 1755.
(25) Rusu, M.; Nicolaescu, I. I.; Rusu, G. G. *Appl. Phys. A* **2000**, *70*, 561.
(26) Rose, D.; Powell, R.; Jayamaha, U.; Maltby, M.; Giolando, D.; McMaster, A.; Kormanyos, K.; Faykosh, G.; Klopping, J.; Dorer, G. *28th IEEE Photovoltaic Specialists Conf*. **2000**, 428.
(27) McCandless, B. E.; Birkmire, R. W.; Buchanan, W. A. *29th IEEE Photovoltaics Specialists Conf*. **2002**, 547.
(28) Abbas Shah, N.; Ali, A.; Ali, Z.; Maqsood, A.; Aqili, A. K. S. *J. Cryst. Growth* **2005**, *284*, 477.
(29) Ali, Z.; Aqili, A. K. S.; Maqsood, A.; Akhtar, S. M. J. *Vacuum* **2005**, *80*, 302.
(30) Bhattacharya, B. *Semiconductor Opto electronic Devices*, 2nd ed.; Prentice Hall: Upper Saddle River, NJ, 1997.
(31) Margrave, J. E. *The Characterization of High-Temperature Vapors*; John Wiley & Sons Inc.: New York, 1967.
(32) Weast, R. C.; Astle, M. J. *CRC Handbook of Chemistry and Physics*, 62nd ed.; CRC Press Inc.: Boca Raton, FL, 1982.
(33) Chu, T. L. *Sol. Cells* **1988**, *23*, 31.
(34) Kestner, J. M.; McElvain, S.; Kelly, S.; Ohno, T.R.; Woods, L. M.; Wolden, C. A. *Sol. Energy Mater. Sol. Cells* **2004**, *83*, 55.
(35) Swanepoel, R. *J. Phys. E: Sci. Instrum*. **1984**, *17*, 896.
(36) Swanepoel, R. *J. Phys. E: Sci. Instrum*. **1983**, *16*, 1214.
(37) Aqili, A. K. S.; Maqsood, A. *Appl. Opt.* **2002**, *41*, 218.
(38) Schroder, D. K. *Semiconductor Materials and Device Characterization*, 2nd ed.; John Wiley & Sons Inc.: New York, 1988.
(39) Birkmire, R. W.; Mccandless, B. E.; Shafarman, W. N. *Sol. Cells* **1988**, *23*, 115.

CG060217Q